Mining for microbial metabolites associated with disease progression in an age-dependent model of experimental autoimmune encephalomyelitis

Annie Pu*, Naomi M Fettig*, Alexandros Polyzois, Ikbel Naouar, Valeria Ramaglia, Leah S Hohman, Michelle Zuo, Julia Copeland, Donny Chan, Katy Davis, Shirley Yu, Sarah Popple, Gary Chao, Kathy D McCoy, Frank C Schroeder, Jennifer L Gommerman*, Lisa C Osborne*

*These authors contributed equally to this manuscript.

Abstract

People with Multiple Sclerosis (pwMS) exhibit alterations in the gut microbiome and its associated metabolites. Identifying causal links between specific fecal microbiome-derived metabolites and disease susceptibility has been shown using fecal microbial transfer (FMT) into animal models of MS (experimental autoimmune encephalomyelitis, EAE). However, a pipeline that identifies microbiome-associated metabolites that can alter age-dependent disease progression is lacking. We recently established a mouse model of MS disease progression that is induced by adoptive transfer of T_H17 cells from young SJL/J mice immunized with myelin peptide into aged recipients. Adapting this model to FMT, we tested the role of young versus aged murine and human fecal microbial communities on disease progression. We demonstrate that microbiota derived from aged SJL/J mice is not sufficient to drive the progressive disease phenotype in young mice. However, human fecal microbiota from young versus aged donors induced a range of EAE phenotypes. Taking advantage of this variability, we were able to identify fecal communities that promote an "aged EAE" phenotype in chronologically young mice that were associated with distinct microbiota-derived metabolites. Our findings provide a framework for metabolite discovery associated with EAE disease chronicity and severity.

Background:

Most relapsing-remitting MS patients ultimately develop a progressive form of the disease which is characterized by increasing disability and cognitive decline (reviewed in Ziemssen et al., 2022). A major risk factor of MS progression is aging (Koch et al., 2007; Tutuncu et al., 2012). Physiological aging is a highly complex and multifaceted process that is influenced by both host intrinsic and extrinsic environmental factors. The gut microbiome, the community of bacteria, fungi, and viruses that symbiotically inhabit the gastrointestinal tract, is a sentinel for both external and internal inputs and has been shown to change with age (reviewed in Ghosh et al., 2022). Some microbial taxa have been consistently associated with unhealthy aging; however, it remains challenging to determine whether microbial changes are a cause or consequence of age-associated comorbidities. Furthermore, increasing evidence indicates that the gut microbiome is altered in people with neurodevelopmental conditions and depression as well as age-related neurological dysfunction such as MS, Alzheimer's disease, Parkinson's disease (reviewed in Ullah et al., 2023 and Fang et al., 2020). The gut microbiota can exert effects at multiple tissues distant from the gastrointestinal tract, including the brain, via microbiota-dependent metabolites (Erny et al., 2015; Rothammer et al., 2016).

A growing body of evidence has shown that fecal microbiome community structure in pwMS (pwMS) differs considerably from that of healthy controls (Jangi et al., 2016; Tremlett et al., 2016; Chen et al., 2016; Miyake et al., 2015; Cantarel et al., 2015; Cox et al., 2021; Cosorich et al., 2017) and healthy household controls (iMSMS Consortium, 2022). Using fecal microbiota transplant (FMT), whereby donor microbial communities from pwMS or controls was introduced into mice lacking an endogenous gut microbiome, a causal connection between MS gut microbiota and incidence of disease in an animal model of MS (experimental autoimmune encephalomyelitis, EAE) has been demonstrated (Cekanaviciute et al., 2017; Berer et al., 2017). How the microbiome, and particularly the aged microbiome, impacts age-dependent disease progression in pwMS is not known.

We have established an EAE model that recapitulates several key pathological features of disease progression (Lassman, 2013) that is induced by adoptive transfer of encephalitogenic Th17 cells into aged SJL/J mice. Compared to young mice, aged SJL/J EAE mice exhibit a protracted clinical disease and enhanced immune infiltration into the CNS, demyelination, cortical grey matter atrophy, and gliosis (Zuo et al., 2022). Here, we demonstrate that aging alone is not a primary driver of microbiome divergence in SJL/J mice, nor does it account for the age-dependent, progressive-like EAE phenotype we have previously described in this strain. Taking advantage of age-dependent differences in human microbial communities, we observed that FMT from an aged human has the capacity to alter the EAE phenotype of young mice to resemble aged mice, and this could be attributed in part to differences in microbiome-derived metabolites. We propose that human FMT experiments in the SJL/J EAE model have the potential to unveil metabolites that promote, or could be used to halt, disease progression.

Results:

The aged SJL microbiome does not drive the age-associated EAE phenotype.

Prior to examining whether an ageing mouse microbiome could account for the severe progressive EAE phenotype observed in aged mice, we tested the impact of ageing on the SJL/J mouse microbiome. Some studies have demonstrated age-dependent changes in the C57BL/6 microbiota (Langille et al., 2014; Boehme et al., 2021; Binyamin et al., 2020; D'Amato et al., 2020), but this has not been examined in SJL mice that typically have a shorter life-expectancy (Yuan et al., 2009). To do this, we collected fecal pellets from cohorts of young and aged SJL/J mice with varying levels of environmental control at two different vivaria, University of Toronto (UofT) vs University of British Columbia (UBC). First, we compared young SJL/J mice (6-8 weeks old) purchased from Envigo (EV) and recently imported into the UofT animal facility against two cohorts of mice that had been purchased from Envigo at a young age and subsequently aged at UofT (8 months old). We also compared young and aged mice bred in-house (IH) at UBC but arising from different breeding pairs. Finally, to account for potential maternal microbiota effects (Moon et al., 2015), we compared young and aged mice born from the same dam (SD), i.e. siblings that are multiple litters apart, at the UofT. Cohorts described are summarized in Figure 1A.

16S rRNA gene sequencing was performed on total fecal DNA. In agreement with some previously published studies in C57Bl/6 mice (Binyamin et al., 2020; Boehme et al., 2021; D'Amato et al., 2020), but not others (Lee et al., 2020; Wu et al., 2021), Shannon alpha diversity did not change between young and aged

SJL/J mice (Figure 1B, left). However, a small increase in the total number of distinct amplicon sequence variants (ASVs) were observed in the EV cohort (Figure 1B, right). Independent of age, fecal microbiomes from EV mice exhibited significantly higher Shannon alpha diversity compared to that of SD and IH groups. In contrast, despite housing at 2 different vivaria, fecal microbiomes from the SD and IH cohorts exhibited similar Shannon diversity and number of observed ASVs, suggesting a potential vendor-dependent effect on this parameter (Figure 1C).

Two dominant phyla represented in mouse gut microbiota are Bacteroidota (formerly Bacteroidetes) and Bacillota (formerly Firmicutes), and the ratio between these phyla has been reported to decrease during human aging (Mariat et al., 2009). Calculation of the Bacillota/Bacteroidota ratio (Blt/Btd ratio) revealed that only young EV mice harbored a significantly higher Blt/Btd ratio compared to all other groups (Figure 1D, 1E). There were no other age-dependent patterns observed in Pseudomonadota (formerly Proteobacteria), Actinobacteriota, Deferribacterota, Desulfobacterota, or Cyanobacteria (data not shown).

Next, the relative abundance of the 20 most abundant families were assessed in all cohorts (Figure S1). The most abundant aggregated families detected in our sequencing include Lachnospiraceae which comprised between 18.2% - 54.7% of reads, Muribaculaceae which comprised between 8.6% - 41.3% of reads, and Rikenellaceae which comprised between 7.1% - 20.2% of reads. Across these families and the remaining 17 most abundant families, there were no generalizable, consistent patterns observed across all cohorts indicative of an age-dependent effect.

Beta diversity was assessed by principal coordinate analysis (PCoA) of Bray-Curtis distances (Figure 2A). An overall significant difference was observed by permutational multivariate ANOVA (PERMANOVA) ($p = 0.001$, permutations = 9999). EV young and aged mice were significantly different in composition (Figure 2B), though this may be partially due to the wide dispersion observed in these groups compared to the other cohorts (Figure 2C). Furthermore, this effect cannot necessarily be attributed to aging as information regarding housing and breeding of these mice at the vendor facility is lacking. Relative to EV mice, all SD mice raised in the UofT vivarium grouped closely together, indicating a high degree of structural similarity among young and aged samples. No differences in dispersion were observed in SD1 or SD2. Overall, these data indicate that under controlled conditions, age alone has a moderate effect on the microbiome of laboratory SJL/J mice, and that Shannon alpha diversity and Blt/Btd ratio are higher in mice directly imported from Envigo (EV) compared to mice reared within either the UofT or UBC facilities.

While the 16S data establish that ageing does not greatly impact microbiome composition, it is possible that minor taxa differences, or taxa that were not sequenced due to their exclusion from the fecal pellet, may nevertheless impact an age-dependent phenotype such as SJL/J adoptive transfer EAE (Zuo et al., 2022). To test this possibility, donor female SPF SJL/J mice were immunized with a peptide derived from myelin proteolipid protein ($PLP_{139-151}$), after which cells from spleens and lymph nodes were collected and re-stimulated *in vitro* with the same PLP peptide under T_H17 skewing conditions (further detailed in Methods). EAE was induced by adoptively transferring cells obtained from these cultures into young vs aged 'siblings' derived from the same dam, and clinical scores were followed for up to 25 days in both sets of SD mice (Figure 3A, 4B). Despite the high degree of similarity in microbiome alpha and beta diversity in these young and aged SD mice, an age-dependent effect outcome on EAE disease course that resembled what we have previously reported in vendor-derived young vs aged mice (Zuo et al., 2022) was still apparent.

We next asked whether an aged microbiome can exacerbate EAE in young mice, and vice versa. To address this question, we performed fecal microbiota transplants (FMT) into germ-free (GF) mice. The donor

microbiota were derived from the cecal contents of young or aged SPF donors that were born and raised in-house and were transferred into sex-matched young or aged GF recipients (Figure 4A). To evaluate if the donor microbiota introduced age-associated changes in the microbiota of recipients, fecal pellets were collected prior to EAE and 16S sequences were compared across groups. Alpha diversity appeared to be higher in both young and aged donor caecal material than in recipient fecal samples (Figure 4B), suggesting incomplete colonization of the donor material, as is common with FMT. In mouse recipients, we observed a trending decrease in alpha diversity in aged recipients of aged FMT compared to young recipients of young FMT and (Figure 4B), possibly due to changes in re-engraftment with host age (Laubitz et al., 2021). The young FMT into young recipients group also exhibited a slightly higher Blt/Btd ratio compared to other groups (Figure 4C). Microbiota compositions largely overlapped by PCoA analysis (Figure 4D). There was a modest but statistically significant difference in Bray-Curtis dissimilarity when mice were aggregated by age of recipient (p = 0.004), by age of donor material (p = 0.001), and between all four experimental groups except when comparing young recipients of young and aged donor material (Table 1). Using differential abundance testing, we detected several significant differences in taxa abundance when mice were grouped by FMT donor (Figure 4E). A full list of differentially abundant taxa is available in Table 2.

This modest shift in microbiota from the FMT, however, did not result in any differences in EAE outcomes. Aged GF recipients adopted a chronic disease phenotype regardless of the age of the transferred microbiota; likewise, young recipients had a reduction in disease severity over time independent of the age of the transferred microbiota (Figure 4F). Across two experiments, only the young FMT into young recipients group did not exhibit any mortality across 21 days of EAE (Figure 4G), although this did not reach statistical significance. Clinical EAE scores at experimental endpoint were significantly higher in aged recipients than in young recipients in both FMT conditions, and young mice remitted to similar degrees regardless of FMT (Figure 4H). The area under the curve (AUC) was calculated as a measure of overall disease severity, which revealed a significant effect of the age of the recipient, but not the FMT age (Figure 4I). These clinical data suggest that differences in mouse microbiota are insufficient to alter age-dependent progressive EAE.

Human stool samples can elicit age-dependent differences in FMT recipient mice.

While we demonstrated that age does not impact the composition of the mouse microbiome, humans exhibit significant shifts in microbiota composition as they age (reviewed in Ghosh et al., 2022). We therefore hypothesized that some human aged microbiomes may increase disease severity in our SJL/J adoptive transfer EAE model, and if so, this may be a better approach for mining for age-dependent metabolites that have the potential to promote disease progression. To test this, we generated microbiome "humanized" mice via FMT, selecting sex-matched, first-degree relative adult donor pairs living in the same household. These pairs were separated in age by at least 25 years (Methods Table 1). This design has previously been validated to improve statistical power in population microbiome studies, and importantly has shown that household variation is a larger contributor to microbial variation than age alone (iMSMS Consortium 2020; 2022). Thus, our study design provides control over some environmental confounders, allowing us to query the effects of age more directly at an individual level. As we did not pre-screen donors based on microbiota-modifying lifestyle factors, substantial variability amongst donor samples was expected.

FMT from four donor pairs were evaluated in young recipient mice, sex-matched to the sex of the FMT donor, for their ability to promote progressive EAE in young mice, evaluating donor slurries independently at

both UofT and UBC sites. Prior to induction of EAE, fecal pellets were taken from FMT recipient mice for 16S analysis. To varying degrees, each pair of FMT donor materials elicited distinct bacterial communities in the recipient mice (Figure 5A-D, left) (by PERMANOVA, $p = 0.001$, permutations = 999). Following FMT engraftment, EAE was induced using $PLP_{139-151}$-primed cells from female donor mice. Aged FMT from donor pair 1 consistently exacerbated EAE and blunted remission compared to the young FMT (Figure 5A). This finding was replicated at both UofT and UBC vivaria using the same donor material (Figure S2). Similarly, although to a lesser extent, aged FMT from donor pair 2 exacerbated EAE by delaying and blunting remission (Figure 5B). However, this phenomenon was not universal across all human donor pairs tested (Figure 5C, 5D). Collectively these data suggest that although age-associated microbiota exist in human donors and are maintained in xenobiotic transplants, not all microbiota communities are capable of modulating progressive MS-like disease.

Mice that received FMT from donor pair 1, which had the most striking difference in clinical disease course, also exhibited significantly different engrafted fecal microbiomes by Bray-Curtis (Figure 5A). To investigate potential drivers of disease enhancement with aged FMT from donor pair 1, we examined differentially abundant taxa in recipient mice. Of 723 taxa tested, a total of 53 met the adjusted p value threshold of less than 0.00001 (Figure S3A). Taxa of potential interest are highlighted in Figure S3B. Taxa significantly higher in the aged FMT include *Fusobacterium ulcerans* (ASV-184), *Parabacteroides merdae* (ASV-474), *Bacteroides caccae* (ASV-444), and two distinct *Bacteroides* species (ASV-428, ASV-430). Conversely, taxa significantly higher in young FMT mice include *B. uniformis* (ASV-427), *B. nordii* (ASV-434), *Bilophila wadsworthia* (ASV-696), *Akkermansia muciniphila* (ASV-424), and an unannotated *Bacteroides* species (ASV-434). A full list of all significantly different taxa is presented in Table 3.

EAE-enhancing microbiota FMT alters metabolomic profile in the CNS.

Post-acute phase disease severity of EAE in young vs aged mice is associated with alterations in meningeal-infiltrating cells that are not T cells (which were separately primed in a donor animal). Since we observed differences in the post-acute phase of EAE in response to the aged but not young participant from donor pair 1, we reasoned that this FMT-dependent phenotype was likewise affecting the CNS rather than the periphery, perhaps through blood-born metabolites that are differentially induced by the transplanted aged human microbiota. We therefore performed untargeted metabolomics on serum and the brain cortex of recipient mice 4-5 weeks post-FMT (Figure 6A). We identified a substantial number of metabolites in mice that received FMT from young vs aged donors of pair 1, with 39 over-represented and 37 under-represented metabolites in the young FMT serum, and 53 over- and 31 under-represented metabolites in the young FMT cortex. Annotated hits determined to be differentially abundant in serum or cortex samples are shown in Figure 6B and 6C. Hits of interest include indole-3-propionic acid (a derivative of tryptophan produced by gut microbiota), equol, and dihydrodaidzein (two intermediate products of daidzein metabolism likely originating from soy products). Other metabolites that do not necessarily originate from environmental sources include isopropylaminopropanoic acid and lauramidopropyl betaine (Figure 6D, 6E). The different metabolomic profiles conferred by gut microbiota may mechanistically explain EAE enhancement observed in aged FMT mice.

Discussion:

In this study, using age-disparate progeny from the same dam or mice aged in a consistent vivarium environment we found that aging (up to 8 months of age) does not greatly impact the composition or diversity of the SJL/J fecal microbiome. Moreover, heterochronic mouse-to-mouse FMT demonstrated that an aged mouse microbiome was insufficient to confer the progressive MS-like phenotype associated with chronological age in young SJL/J mice and vice versa. In contrast, FMT of microbiota from some aged human donors was able to confer an aged EAE phenotype in young SJL/J mice. Chronologically young recipient mice colonized with an aged human donor microbiota that reliably induced an aged EAE phenotype demonstrated significant alterations in the metabolome of their blood and cortex. Collectively, these results provide new insights into limitations of using mouse FMT for aging studies and demonstrate that applying human FMT to our novel EAE model provides a mechanism for unveiling metabolites that alter disease progression.

A myriad of confounding factors must be considered when conducting microbiome studies in mice (Macpherson & McCoy, 2015). The major determinants of mouse gut microbiota composition are vertical inheritance, vivarium-dependent factors such as diet, water acidification, light cycle and handling, and genetic differences among strains or genetically-modified strains (Parker et al., 2018; Long et al., 2021; Rasmussen et al., 2019; Guo et al., 2022; Moeller et al., 2018; reviewed in Stappenbeck & Virgin, 2016). Furthermore, vendor-to-vendor differences in microbiome composition and strain genetics are notorious for their impact on the immune response and by extension, on disease models such as EAE (deLuca et al., 2010; Ivanov et al., 2009; reviewed in Alegre, 2019). When these factors are controlled to the best of our ability, we did not observe a major impact of age on microbiome composition or diversity in SJL/J mice.

Alternatively, humans experience a wide variety of environmental exposures that modify gut microbiota which are absent in the vivarium (e.g. dietary changes, infection history, circadian rhythm disruptions, environmental pollutants, antibiotic exposure, and other lifestyle choices). Thus, FMT from human donors has the capacity to introduce some of the complexities that arise in the microbiome over the course of a lifetime. Our approach of recruiting pairs of first-degree relatives that share the same sex and household limits the genetic and environmental confounders between them and allows greater confidence in identifying microbes and their associated metabolites that may be altered by age.

We have identified differentially abundant taxa present in FMT donor material that are associated with exacerbated disease. Whether these changes are due to age alone is still under speculation, as we did not collect dietary or lifestyle information and only pre-screened donors based on general daily health. Prominently, the high abundance of *Akkermansia muciniphila* found in young FMT may be one mechanism of protection in EAE, as *A. muciniphila* has been linked in multiple reports to be a tolerogenic species (Gandy et al., 2019; Cekanaviciute et al., 2017; Cox et al., 2021). Short-chain fatty acid producers such as *Roseburia* species were also enriched in young FMT mice. *Parabacteroides merdae* and *Ruminococcus gnavus* have been found to be enriched in elderly individuals (Yan et al., 2022; Wang et al., 2019).

Furthermore, we found that the different microbial communities introduced into experimental mice also conferred distinct metabolomic profiles in both the serum and cortex. Several metabolites have been identified as particularly enriched in either the young or aged FMT mice, some of which have specific relevance to the gut-brain axis. These were indole-3-propionic acid (IPA), equol, and dihydrodaidzein. IPA is one of several indole derivatives that is produced solely by tryptophan metabolism by bacteria. This family of

indole compounds have already been implicated in both CNS and non-CNS diseases, but IPA in particular has been shown to be important in maintaining gut barrier integrity and exhibit immunomodulatory activity, possibly through either the pregnane X receptor or aryl hydrocarbon receptor (Venkatesh et al., 2014; Rothhammer et al., 2016; Huang et al., 2022). Furthermore, age-associated declines in serum tryptophan and indole levels have been reported in both mice and humans (Wu et al., 2021; Ruiz-Ruiz et al., 2020). Equol and dihydrodaidzein are both derived from intestinal processing of isoflavones found in legumes, and their reciprocal abundance in young and aged FMT mice may indicate a deficiency in the ability of the gut microbiota to process dihydrodaidzein into equol. The functional implications of the lack of equol in EAE are still unclear, however equol has been reported to be neuroprotective (Subedi et al 2017). Interestingly, our 16S sequencing efforts also identified an enrichment in *Adlercreuzia equolifaciens*, a known equol producer, in young FMT mice (Maruo et al., 2008).

There are some limitations to our study. Although the EAE phenotypes observed in this study were highly reproducible across independent investigators at geographically separated vivariums, several technical steps - the processing of the donor material, the number of "doses" the recipient mice are exposed to, and the recipient gut environment (i.e., housing, age, strain), impact FMT colonization. Additionally, the human-to-mouse FMT portion of this study was limited to four pairs of self-reportedly healthy human donors, and for the scope of this study we specifically excluded individuals with any diagnosed chronic health conditions. This may explain, in part, why we observed that aged FMT donors did not universally modify EAE in mice. There is also insufficient power to draw conclusions regarding patterns in aging microbiota or metabolites, but it is perhaps promising that not all microbiotas derived from aged donors had disease-enhancing potential. Nevertheless, since our FMT pipeline introduces human-adapted microbes that elicit disparate EAE phenotypes, our approach offers a translationally relevant pipeline to mine for metabolites for treatment MS progression.

Methods:

Animals

All experiments were performed in accordance with the ethical guidelines of the Animal Care Committees at the University of British Columbia (UBC) and University of Toronto (UofT). Conventional female or male SJL/J mice were either purchased from Envigo, USA (SJL/JCrHsd) or bred in-house at UBC or UofT (as specified in figure legends). Unless stated otherwise, all young mice used are 6-14 weeks of age, and aged mice are 8-12 months of age and age-matched across experimental groups. 12 months is the maximum age for aged mice due to high incidence of tumors in older mice (Crispens, 1973).

At UBC in the Centre for Disease Modeling, mice were housed up to 5 mice per cage in ventilated Ehret cages prepared with BetaChip bedding and had *ad libitum* access to food (PicoLab Diet 5053) and water (reverse osmosis/chlorinated (2-3ppm)-purified). Housing rooms were maintained on a 14/10-hour light/dark cycle with temperature and humidity ranges of 20-22°C and 40-70%, respectively. Sentinel mice housed in experimental rooms were maintained on dirty bedding and nesting material and were tested on a quarterly basis for presence of mites (*Myocoptes, Radford/Myovia),* pinworm (*Aspiculuris tetaptera, Syphacia obvelata)*, fungi (*encephalitozooan cuniculi)*, bacteria (*Helicobacter spp., Clostridium piliforme, Mycoplasma pulmonis,*

CAR Bacillus), and viruses (Ectromelia, EDIM/Rotavirus, MHV, MNV, MVM, LCMV, MAV1/2, MCMV, Polyoma, PVM, REO3, Sendai, and TMEV).

At UofT in the Center for Cellular and Biomolecular Research, animals were housed under SPF conditions, up to 4 mice per cage in ventilated Allentown cages prepared with bedding, nesting material, and enrichment. All mice had *ad libitum* access to 18% protein rodent diet (Teklad 2918) and acidified water. Housing rooms were maintained on a 12/12-hour light/dark cycle, temperatures of 20-26°C, and humidity of 35-70%. Sentinel animals were housed in similar conditions and tested quarterly for mites and pinworm in addition to MHV, MVM, NS1, MPV, MNV, TMEV, and EDIM, and annually for Sendai, *M. pulmonis*, PVM, REO3, LCMV, Ectro, and MAV1/2.

Germ-free SJL/J mice were generated through rederivation via in vitro fertilization of germ-free pseudopregnant females at the International Microbiome Centre (University of Calgary) and bred at UofT and UBC. GF mice were bred and housed in sterile vinyl isolators (Class Biologically Clean, Madison WI). At UBC, fecal pellets were sampled every 2 weeks to verify sterility by aerobic and anaerobic culturing, and monthly by 16S qPCR. For FMT studies, GF mice were transferred to Ehret cages, gavaged immediately with prepared samples and then housed under SPF conditions. At UofT, GF mice were bred and housed in either Tecniplast ISOcage™ cages or semi-rigid isolators. Fecal pellets were sampled every 2 weeks for monitoring germ-free status by culture or PCR for detection of bacterial 16S rRNA and fungal 18S and 28S ITS.

<u>16S rRNA gene sequencing</u>

Fresh fecal pellets from animals were collected either directly from live animals or from the distal colon at experimental endpoints. Pellets were stored at -20°C until use. Remaining human donor material was also refrozen at -20°C after thawing once for oral gavage. DNA extraction was performed using the Macherey-Nagel NucleoSoil kit according to manufacturer instructions, and DNA quality was assessed using NanoDrop. Samples that met a minimum value of 1.8 for $OD_{260/280}$ were considered sufficiently pure for sequencing.

Sequencing was performed at the Center for Analysis of Genome Evolution and Function. The V4 hypervariable region of the 16S rRNA gene was amplified using uniquely barcoded 515F (forward) and 806R (reverse) sequencing primers (Caporaso et al., 2012). The V4 region was amplified by cycling the reaction at 95°C for 3 minutes, 18x cycles of 95°C for 15 seconds, 50°C for 15 seconds and 72°C for 15 seconds, followed by a 5-minute 72°C extension. All amplification reactions were done in duplicate to reduce amplification bias, pooled, and checked on a 1% agarose TBE gel. Pooled duplicates were quantified using PicoGreen and combined by even concentrations. The library was then purified using Ampure XP beads and loaded on to the Illumina MiSeq for sequencing, according to manufacturer instructions (Illumina, San Diego, CA). Sequencing was performed using the V2 (150bp x 2) chemistry. A single-species (*Pseudomonas aeruginosa* DNA), a mock community (Zymo Microbial Community DNA Standard D6305), and a template-free negative control were included in the sequencing run.

The dada2 pipeline was used for inferring amplicon sequence variants (ASVs) from individual fastq files. Briefly, the final 10 bases of all sequences were trimmed, and default filtering parameters for dada2 were used for denoising (maxN = 0, trunQ = 2, and maxEE = 2). Merging of paired reads, construction of an ASV table, and removal of chimeras were all performed through the dada2 pipeline. Taxonomy assignment was performed through the use of the Silva 138.1 NR99 reference database. dada2 outputs (ASV table, taxonomy table) and sample metadata were combined and analyzed further using the phyloseq package. ASVs not

assigned to a known phylum and low prevalence taxa were removed prior to all downstream analyses. R packages used are listed in Methods Table 3.

Mouse cecal material processing

Whole ceca from young or aged mice were collected in sterile 1.5 mL collection tubes and either snap-frozen on dry ice and stored at -80°C or moved immediately to an anaerobic chamber for processing. Individual ceca were transferred to a sterile homogenization tube with metal bead containing 500 µL sterile, pre-reduced PBS. Ceca were homogenized in a bead beater homogenizer for 5 minutes at 1800 rpm. Homogenate was filtered through a 70 µm nylon filter to remove debris. If several donor ceca were collected, cecal material was pooled into an age- and sex-matched batch. The cecal suspension was diluted to a total volume of 2 mL PBS per cecum. Suspensions were aliquoted into 1 mL cryovials and resuspended in 15% glycerol for storage at -80°C.

Human fecal material processing

Stool samples were collected from donors on site at UofT. All pairs of donors were required to have been born in Canada or immigrated 10+ years prior, be cohabitating for the past 5 years, be disparate in age by 25 years, be of the same sex, and be direct relatives. Stool was deposited into 50 mL collection tubes, and either stored at -80°C or moved into an anaerobic chamber (5% H_2, 5% CO_2, 90% N_2) for immediate processing. All reagents used inside the anaerobic chamber were pre-sterilized. An aliquot of stool was weighed and deposited into a fresh 50 mL conical tube, and sterile 0.3 mm glass beads were added. Sterile, pre-reduced PBS was added at 10 mL per 1 g of stool. Stool was gently vortexed in short bursts until homogenized, then poured through a 0.25 mm metal strainer to remove glass beads and large particles. Filtered homogenate was centrifuged at 5000 x *g* for 20 minutes at room temperature. Supernatant was discarded, and the pellet was weighed and resuspended at 10 mL of 15% glycerol in PBS per gram. Samples were transferred to -80°C as 1 mL aliquots for storage.

Methods Table 1: Human FMT material donors

Donor ID	Sex	Age Difference (years)
Pair 1	Male	25
Pair 2	Female	29
Pair 3	Male	30
Pair 4	Female	29

Antibiotic treatment and FMT

SPF-housed SJL/J mice were microbiome-depleted using antibiotic cocktails as previously described (Staley et al., 2017). Briefly, antibiotics were added to animal facility drinking water, each at 1 mg/mL. A "non-absorbable" cocktail (ertapenem, neomycin, vancomycin) was administered for 7 days, followed by a 2-day wash-out with regular drinking water. Next, a "systemic" cocktail (ampicillin, cefoperazone, clindamycin) was administered for 7 days, followed by a 2-day washout with regular drinking water. A final round of "non-absorbable" cocktail was administered for 7 days, followed by a 2-day wash-out period prior to fecal/cecal microbiota transplant. Antibiotic-treated mice were orally gavaged with 200 µL of donor material (fecal material from human donors and cecal material from mouse donors, all herein referred to as "FMT"). Young germ-free mice were each given 100 µL of donor material, as they received the FMT at a younger age than

conventional mice (5-6 weeks old vs 9-10 weeks old), and thus were smaller in size compared to conventional mice. Animals were transferred from standard SPF GF housing to CL2 housing at the time of oral gavage, which is maintained with the same environmental conditions described above. Transferred microbiome was allowed to settle for for 3-4 weeks following oral gavage to allow microbiota colonization prior to any further experimental procedures.

Passive experimental autoimmune encephalomyelitis

Immunization of female donor mice aged 7-9 weeks old was achieved using an emulsion containing 100 µg $PLP_{131-159}$ and 200 µg *Mycobacterium* suspended in incomplete Freund's adjuvant (IFA) and PBS. Donor mice were injected subcutaneously with 100 µL of emulsion at each hind flank and at the neck (UofT) or one injection in the hind flank (UBC). On day 9 following immunization, donor animals were euthanized and inguinal, axillary, brachial, and superficial cervical lymph nodes and spleens were harvested. For restimulation in culture, lymph nodes and spleens were mashed directly through a 70 µm filter into sterile ice-cold PBS. Cells were washed, counted, and resuspended in culturing media. Cells were transferred into culture flasks at 2.5×10^8 cells per T-75 flask, in a final volume of 50 mL of media per flask. Cells were cultured for 72 hours at 37°C, 5% CO_2 in the presence of 10 µg/mL $PLP_{139-151}$, 10 ng/mL rIL-23, 20 µg/mL αIL-4, and 20 µg/mL αIFNg. Details of relevant reagents are listed in Methods Table 2.

Culture media: RPMI appended with 10% (v/v) FBS, 1% (v/v) GlutaMAX™, 1 mM sodium pyruvate, 1% (v/v) non-essential amino acids, 100 U/mL Penicillin-Streptomycin, and 55 µM β-mercaptoethanol.

After 72 hours, cells were collected from flasks and washed. For injection into recipient mice, cells were resuspended at 1.0×10^8 cells/mL. Recipient mice were either injected with 1.0×10^7 or 2.0×10^7 cells (indicated where relevant) intraperitoneally. Mice were monitored for up to 25 days, and disease scores and body weight measurements were taken daily. For supportive care starting 4-5 days after adoptive transfer, cage bedding was switched to Pure-o'Cel material and cages were placed on heat pads set to 37°C. One (1)-3 subcutaneous injections of Ringer's lactate solution were given based on degree of dehydration, and wet mash using powdered 19% protein rodent chow (Teklad, 2919) or DietGel Recovery (Clear H_2O) was supplied in cages and refreshed daily. For paralyzed animals, bladders were gently expressed daily 1-3 times, as needed.

Sample preparation for metabolomic analysis

For metabolite extraction, whole, snap-frozen mouse serum, cecal content, fecal pellet, cortex, and leptomeninges samples were processed as follows. Frozen cortex samples were crushed and ground into a fine powder with a pre-chilled mortar and pestle, with dry ice added throughout to prevent sample thawing. Then, 10 µL methanol was added per mg of powdered sample, and samples were sonicated for 5 min. Extracts were pelleted at 5,000 g for 5 min, and supernatants were transferred to another 20 mL glass vial. Remaining pellets were further extracted with another 10 min of vigorous stirring in 5 mL ethanol. The supernatants were combined and then dried in a SpeedVac (ThermoFisher Scientific) vacuum concentrator. Dried materials were resuspended in 300 µL of methanol. Samples were pelleted at 5,000 g for 5 min and clarified extracts were transferred to fresh HPLC vials and stored at −20 °C until analysis.

For the analysis of both donor and mice serum samples, 400 µL of methanol was added per 100 µL of sample. The samples were vortexed and centrifuged, and supernatant was collected. An additional volume of 200 µL of methanol was added to the residue and the vial was again vortexed and centrifuged. The combined

supernatants were dried in a SpeedVac (ThermoFisher Scientific) vacuum concentrator. Samples were resuspended in 50 µL of methanol and pelleted at 5,000 g for 5 min. Clarified extracts were transferred to fresh HPLC vials and stored at −20 °C until analysis.

Mass spectrometric analysis

HPLC-HRMS analysis was conducted using a Thermo Fisher Scientific Vanquish Horizon ultra-HPLC (UHPLC) System coupled to a Thermo Q Exactive hybrid quadrupole-orbitrap high-resolution mass spectrometer equipped with a heated electrospray ionization (ESI) ion source, using Thermo Scientific Xcalibur software (v.4.3.73.11). For each sample, 1 µL of the above prepared methanol extracts was injected and separated using a water-acetonitrile gradient on a Thermo Scientific Accucore C18 column (150 × 2.1 mm, 1.5 µm particle size) and maintained at 40°C. Optima grade solvents were purchased from Fisher Scientific. Solvent A was 0.1% formic acid in water and solvent B was 0.1% formic acid in acetonitrile. A/B gradient started at 1% B for 3 min, then increased linearly to 98% B at 20 min, followed by 98% B for 5 min, then down to 1% B for 3 min. Mass spectrometer parameters: +3.5 kV spray voltage, 380°C capillary temperature, 40°C probe heater temperature, 60 AU sheath flow rate, 20 AU auxiliary flow rate, 2 AU sweep gas; S-lens radio frequency level 50.0, resolution 60,000 at m/z 200, m/z range 80–1,200, AGC target 3E6. Normalized collision energy was set to a stepwise increase from 10 to 30 to 50 % with z = 1 as default charge state. For MS2 data analysis, raw spectra were converted to .mzXML files using MSconvert (ProteoWizard). MS1 and MS2 feature extraction was performed using MZmine 3.4.14 (Schmid, R et al. 2023). The output was further processed through GNPS for molecular networking and library matching. The parameters used in MZmine3 and GNPS (Wang, M.et al. 2016) are listed in table below. Chemical feature prioritization and identification of chemical drivers was performed using Metaboseek (Helf, M.J et al. 2022), applying filters on fold change with threshold 3 and p-value with threshold 0.05.

Statistics

Data visualizations and statistical analysis were performed either using GraphPad Prism or RStudio. Relevant statistical tests are specified in figure captions. Relevant R packages are described in Methods Table 3.

Methods Table 2: Reagents

Purpose/Reagent	UBC	UofT
Antibiotics		
Ertapenem	Invanz® (ertapenem sodium, Merck) Ertapenem sodium (generic)	Invanz® (ertapenem sodium, Merck)
Neomycin	Neomycin trisulfate salt hydrate (Sigma, N6386)	Neomycin sulfate (BioShop, NEO201)
Vancomycin	Vancomycin hydrochloride (Chem-Impex Intl., 00315)	Vancomycin hydrochloride (BioShop, VAN990)
Ampicillin	Ampicillin trihydrate (Thermo, J6651422)	Ampicillin sodium salt (BioShop, AMP201)
Cefoperazone	Cefoperazone sodium salt (Sigma, C4292)	Cefoperazone sodium salt (Sigma, C4292)
Clindamycin	Dalacin® C (clindamycin hydrochloride capsules, Pfizer)	Antirobe® (clindamycin hydrochloride solution, Zoetis)
EAE		
$PLP_{139-151}$	GenScript (RP10550) CanPeptide	CanPeptide

Mycobacterium	BD Difco	BD Difco
IFA	BD Difco	BD Difco
Cell culture		
rIL-23	R&D Systems (1887-ML-010/CF)	R&D Systems (1887-ML-010/CF)
αIL-4	Bio X Cell (clone 11B11, BE0045)	Bio X Cell (clone 11B11, BE0045)
αIFNg	Bio X Cell (clone XMG1.2, BE0055)	Bio X Cell (clone XMG1.2, BE0055)

Methods Table 3: R packages

Package	**Citation**	**Dataset**	**Purpose**
dada2	Callahan et al., 2016	16S	Pre-processing of raw sequencing data
phyloseq	McMurdie & Holmes, 2013	16S	Handling and analysis of microbiome data
ampvis2	Andersen et al., 2018	16S	Heatmap visualizations
vegan	Oksanen et al., 2022	16S	Statistical comparisons (PERMANOVA, PERMDISP2)
pairwiseAdonis	Martinez Arbizu et al., 2020	16S	Statistical comparisons (PERMANOVA)
tidyverse	Wickham et al., 2019	16S	Plot generation
DESeq2	Love et al., 2014	16S	Differential abundance testing

References

Alegre M-L. Mouse microbiomes: overlooked culprits of experimental variability. Genome Biology. 2019;20.

Andersen, K. S., Kirkegaard, R. H., Karst, S. M., & Albertsen, M. (2018). ampvis2: an R package to analyse and visualise 16S rRNA amplicon data. bioRxiv (Cold Spring Harbor Laboratory).

Berer K, Gerdes LA, Cekanaviciute E, Jia X, Xiao L, Xia Z, et al. Gut microbiota from multiple sclerosis patients enables spontaneous autoimmune encephalomyelitis in mice. Proceedings of the National Academy of Sciences of the United States of America. 2017;114:10719–24.

Biagi E, Rampelli S, Turroni S, Quercia S, Candela M, Brigidi P. The gut microbiota of centenarians: signatures of longevity in the gut microbiota profile. Mechanisms of Ageing and Development. 2017;165;180-184.

Binyamin D, Werbner N, Nuriel-Ohayon M, Uzan A, Mor H, Abbas A, et al. The aging mouse microbiome has obesogenic characteristics. Genome Medicine. 2020;12.

Boehme M, Guzzetta KE, Bastiaanssen TFS, Van De Wouw M, Moloney GM, Gual-Grau A, et al. Microbiota from young mice counteracts selective age-associated behavioral deficits. Nature Aging. 2021;1:666–76.

Callahan, B. J., McMurdie, P. J., Rosen, M. J., Han, A. W., Johnson, A. J. A., & Holmes, S. P. (2016). DADA2: High-resolution sample inference from Illumina amplicon data. Nature Methods, 13(7), 581–583.

Cantarel BL, Waubant E, Chehoud C, Kuczynski J, DeSantis TZ, Warrington J, et al. Gut microbiota in multiple sclerosis: possible influence of immunomodulators. Journal of Investigative Medicine. 2015;63:729–34.

Caporaso JG, Lauber CL, Walters WA, Berg-Lyons D, Huntley J, Fierer N, et al. Ultra-high-throughput microbial community analysis on the Illumina HiSeq and MiSeq platforms. The ISME Journal. 2012;6:1621–4.

Cekanaviciute E, Yoo BB, Runia TF, Debelius JW, Singh S, Nelson CA, et al. Gut bacteria from multiple sclerosis patients modulate human T cells and exacerbate symptoms in mouse models. Proceedings of the National Academy of Sciences of the United States of America. 2017;114:10713–8.

Chen J, Chia N, Kalari KR, Yao JZ, Novotna M, Soldan MMP, et al. Multiple sclerosis patients have a distinct gut microbiota compared to healthy controls. Scientific Reports. 2016;6.

Cosorich I, Dalla-Costa G, Sorini C, Ferrarese R, Messina MJ, Dolpady J, et al. High frequency of intestinal T H 17 cells correlates with microbiota alterations and disease activity in multiple sclerosis. Science Advances. 2017;3.

Cox LM, Maghzi AH, Liu S, Tankou SK, Dhang FH, Willocq V, et al. Gut microbiome in progressive multiple sclerosis. Annals of Neurology. 2021;89:1195–211.

Crispens CG. Some characteristics of strain SJL/JDg mice. Laboratory Animal Science. 1973;23:408-413.

D'Amato A, Di Cesare Mannelli L, Lucarini E, Man AL, Gall GL, Branca JJV, et al. Faecal microbiota transplant from aged donor mice affects spatial learning and memory via modulating hippocampal synaptic plasticity- and neurotransmission-related proteins in young recipients. Microbiome. 2020;8.

deLuca LES, Pikor NB, O'Leary J, Galicia-Rosas G, Ward LA, Defreitas D, et al. Substrain differences reveal novel Disease-Modifying gene candidates that alter the clinical course of a rodent model of multiple sclerosis. ˜the œJournal of Immunology/˜the œJournal of Immunology. 2010;184:3174–85.

Erny D, De Angelis ALH, Jaitin D, Wieghofer P, Staszewski O, David E, et al. Host microbiota constantly control maturation and function of microglia in the CNS. Nature Neuroscience. 2015;18:965–77.

Fang P, Kazmi SA, Jameson KG, Hsiao EY. The microbiome as a modifier of neurodegenerative disease risk. Cell Host & Microbe. 2020;28:201–22.

Gandy KAO, Zhang J, Nagarkatti P, Nagarkatti M. The role of gut microbiota in shaping the relapse-remitting and chronic-progressive forms of multiple sclerosis in mouse models. Scientific Reports. 2019;9.

Ghosh TS, Shanahan F, O'Toole PW. The gut microbiome as a modulator of healthy ageing. Nature Reviews Gastroenterology & Hepatology. 2022;19:565–84.

Guo J, Song C, Liu Y, Wu X, Dong W, Zhu H, et al. Characteristics of gut microbiota in representative mice strains: Implications for biological research. Animal Models and Experimental Medicine. 2022;5:337–49.

Helf MJ, Fox BW, Artyukhin AB, Zhang YK, Schroeder FC. Comparative metabolomics with Metaboseek reveals functions of a conserved fat metabolism pathway in C. elegans. Nature Communications. 2022;13.

Huang ZB, Hu Z, Lu CX, Luo SD, Chen Y, Zhou ZP, et al. Gut microbiota-derived indole 3-propionic acid partially activates aryl hydrocarbon receptor to promote macrophage phagocytosis and attenuate septic injury. Frontiers in Cellular and Infection Microbiology. 2022;12.

Ivanov II, Atarashi K, Manel N, Brodie EL, Shima T, Karaoz U, et al. Induction of intestinal Th17 cells by segmented filamentous bacteria. Cell. 2009;139;485-498.

Jangi S, Gandhi R, Cox LM, Li N, Von Glehn F, Yan R, et al. Alterations of the human gut microbiome in multiple sclerosis. Nature Communications. 2016;7.

Koch M, Mostert J, Heersema D, De Keyser J. Progression in multiple sclerosis: Further evidence of an age dependent process. Journal of the Neurological Sciences. 2007;255:35–41.

Langille MGI, Meehan CJ, Koenig JE, Dhanani AS, Rose RA, Howlett SE, et al. Microbial shifts in the aging mouse gut. Microbiome. 2014;2.

Lassmann H. Pathology and disease mechanisms in different stages of multiple sclerosis. Journal of the Neurological Sciences. 2013;333:1–4.

Laubitz D, Typpo K, Midura-Kiela M, Brown C, Barberan A, Ghishan FK, et al. Dynamics of gut microbiota recovery after antibiotic exposure in young and old mice (a pilot study). Microorganisms. 2021;9.

Lee J, D'Aigle J, Atadja L, Quaicoe V, Honarpisheh P, Ganesh BP, et al. Gut Microbiota–Derived Short-Chain fatty acids promote poststroke recovery in aged mice. Circulation Research. 2020;127:453–65.

Ley RE, Bäckhed F, Turnbaugh P, Lozupone CA, Knight RD, Gordon JI. Obesity alters gut microbial ecology. Proceedings of the National Academy of Sciences of the United States of America. 2005;102:11070–5.

Long LL, Svenson KL, Mourino AJ, Michaud M, Fahey JR, Waterman L, et al. Shared and distinctive features of the gut microbiome of C57BL/6 mice from different vendors and production sites, and in response to a new vivarium. Lab Animal. 2021;50:185–95.

Love, M.I., Huber, W., Anders, S. Moderated estimation of fold change and dispersion for RNA-seq data with DESeq2. Genome Biology. 2014;15.

Macpherson AJ, MCCoy KD. Standardised animal models of host microbial mutualism. Mucosal Immunology. 2015;8;476-486.

Mariat D, Firmesse O, Levenez F, Guimarães V, Sokol H, Doré J, et al. The Firmicutes/Bacteroidetes ratio of the human microbiota changes with age. BMC Microbiology. 2009;9:123.

Martinez Arbizu P. pairwiseAdonis: Pairwise Multilevel Comparison using Adonis. R package version 0.4.1. 2017.

Maruo T, Sakamoto M, Ito C, Toda T, Benno Y. Adlercreutzia equolifaciens gen. nov., sp. nov., an equol-producing bacterium isolated from human faeces, and emended description of the genus Eggerthella. International Journal of Systematic and Evolutionary Microbiology. 2008;58:1221–7.

McMurdie PJ, Holmes S. phyloseq: An R Package for Reproducible Interactive Analysis and Graphics of Microbiome Census Data. PloS One. 2019;8.

Miyake S, Kim S, Suda W, Oshima K, Nakamura M, Matsuoka T, et al. Dysbiosis in the Gut Microbiota of Patients with Multiple Sclerosis, with a Striking Depletion of Species Belonging to Clostridia XIVa and IV Clusters. PloS One. 2015;10:e0137429.

Moeller AH, Suzuki TA, Phifer-Rixey M, Nachman MW. Transmission modes of the mammalian gut microbiota. Science. 2018;362:453–7.

Moon C, Baldridge MT, Wallace MA, Burnham CAD, Virgin HW, Stappenbeck TS. Vertically transmitted faecal IgA levels determine extra-chromosomal phenotypic variation. Nature Letters. 2015;521:90-93.

Oksanen J, Simpson G, Blanchet F, Kindt R, Legendre P, Minchin P, et al. vegan: Community Ecology Package. R package version 2.6-4. 2022.

Parker KD, Albeke SE, Gigley JP, Goldstein AM, Ward NL. Microbiome composition in both Wild-Type and disease model mice is heavily influenced by mouse facility. Frontiers in Microbiology. 2018;9.

Rasmussen TS, De Vries L, Kot W, Hansen LH, Castro-Mejía JL, Vogensen FK, et al. Mouse vendor influence on the bacterial and viral gut composition exceeds the effect of diet. Viruses. 2019;11:435.

Rothhammer V, Mascanfroni ID, Bunse L, Takenaka MC, Kenison JE, Mayo L, et al. Type I interferons and microbial metabolites of tryptophan modulate astrocyte activity and central nervous system inflammation via the aryl hydrocarbon receptor. Nature Medicine. 2016;22:586–97.

Ruiz-Ruiz S, Sanchez-Carrillo S, Ciordia S, Mena MC, Méndez-García C, Rojo D, et al. Functional microbiome deficits associated with ageing: Chronological age threshold. Aging Cell. 2019;19.

Schmid R, Heuckeroth S, Korf A, Smirnov A, Myers O, Dyrlund TS, et al. Integrative analysis of multimodal mass spectrometry data in MZmine 3. Nature Biotechnology. 2023;41;447-449.

Staley C, Kaiser T, Beura LK, Hamilton MJ, Weingarden AR, Bobr A, et al. Stable engraftment of human microbiota into mice with a single oral gavage following antibiotic conditioning. Microbiome. 2017;5.

Stappenback TS, Virgin HW. Accounting for reciprocal host-microbiome interactions in experimental science. Nature. 2016;534:191-199.

Subedi L, Ji E, Shin D, Jin J, Yeo JH, Kim SY. Equol, a dietary daidzein gut metabolite attenuates microglial activation and potentiates neuroprotection in vitro. Nutrients. 2017;9:207.

Tremlett H, Fadrosh DW, Faruqi AA, Zhu F, Hart J, Roalstad S, et al. Gut microbiota in early pediatric multiple sclerosis: a case−control study. European Journal of Neurology. 2016;23:1308–21.

Tutuncu M, Tang J, Zeid NA, Kale N, Crusan DJ, Atkinson EJ, et al. Onset of progressive phase is an age-dependent clinical milestone in multiple sclerosis. Multiple Sclerosis. 2012;19:188–98.

Ullah H, Arbab S, Tian Y, Liu C-Q, Chen Y, Qijie L, et al. The gut microbiota–brain axis in neurological disorder. Frontiers in Neuroscience. 2023;17.

Venkatesh M, Mukherjee S, Wang H, Li H, Sun K, Benechet AP, et al. Symbiotic bacterial metabolites regulate gastrointestinal barrier function via the xenobiotic sensor PXR and Toll-like receptor 4. Immunity. 2014;41:296-310.

Wang M, Carver JJ, Phelan VV, Sanchez LM, Garg, N., Peng Y, et al. Sharing and community curation of mass spectrometry data with Global Natural Products Social Molecular Networking. Nature Biotechnology. 2016;34;828-837.

Wickham H, Averick M, Bryan J, Chang W, McGowan L, François R, et al. Welcome to the Tidyverse. Journal of Open Source Software. 2019;4.

Wu C-S, Muthyala SDV, Klemashevich C, Ufondu AU, Menon R, Chen Z, et al. Age-dependent remodeling of gut microbiome and host serum metabolome in mice. Aging. 2021;13:6330–45.

Wu L, Zeng T, Zinellu A, Rubino S, Kelvin DJ, Carru C. A cross-sectional study of compositional and functional profiles of gut microbiota in Sardinian centenarians. mSystems. 2019;4.

Wu W-L, Adame MD, Liou C-W, Barlow JT, Lai T-T, Sharon G, et al. Microbiota regulate social behaviour via stress response neurons in the brain. Nature. 2021;595:409–14.

Yan H, Qin Q, Yan S, Chen J, Yang Y, Li T, et al. Comparison of the gut microbiota in different age groups in China. Frontiers in Cellular and Infection Microbiology. 2022;12.

Yuan R, Tsaih S-W, Petkova SB, De Evsikova CM, Xing S, Marion MA, et al. Aging in inbred strains of mice: study design and interim report on median lifespans and circulating IFG1 levels. Aging Cell. 2009;8;277-287.

Zhang F, Zhang X, Fu J, Duan Z, Qiu W, Cai Y, et al. Sex- and Age-Dependent Associations between Parabacteroides and Obesity: Evidence from Two Population Cohort. Microorganisms. 2023;11:2087.

Zhou X, Baumann R, Gao X, Mendoza M, Singh S, Sand IK, et al. Gut microbiome of multiple sclerosis patients and paired household healthy controls reveal associations with disease risk and course. Cell. 2022;185:3467-3486.e16.

Zhou X, Singh S, Baumann R, Barba P, Landefeld J, Casaccia P, et al. Household paired design reduces variance and increases power in multi-city gut microbiome study in multiple sclerosis. Multiple Sclerosis. 2020;27:366–79.

Ziemssen T, Bhan V, Chataway J, Chitnis T, Cree BAC, Havrdova EK, et al. Secondary progressive multiple sclerosis. Neurology® Neuroimmunology & Neuroinflammation. 2023;10.

Zuo M, Fettig NM, Bernier L-P, Pössnecker E, Spring S, Pu A, et al. Age-dependent gray matter demyelination is associated with leptomeningeal neutrophil accumulation. JCI Insight. 2022;7.

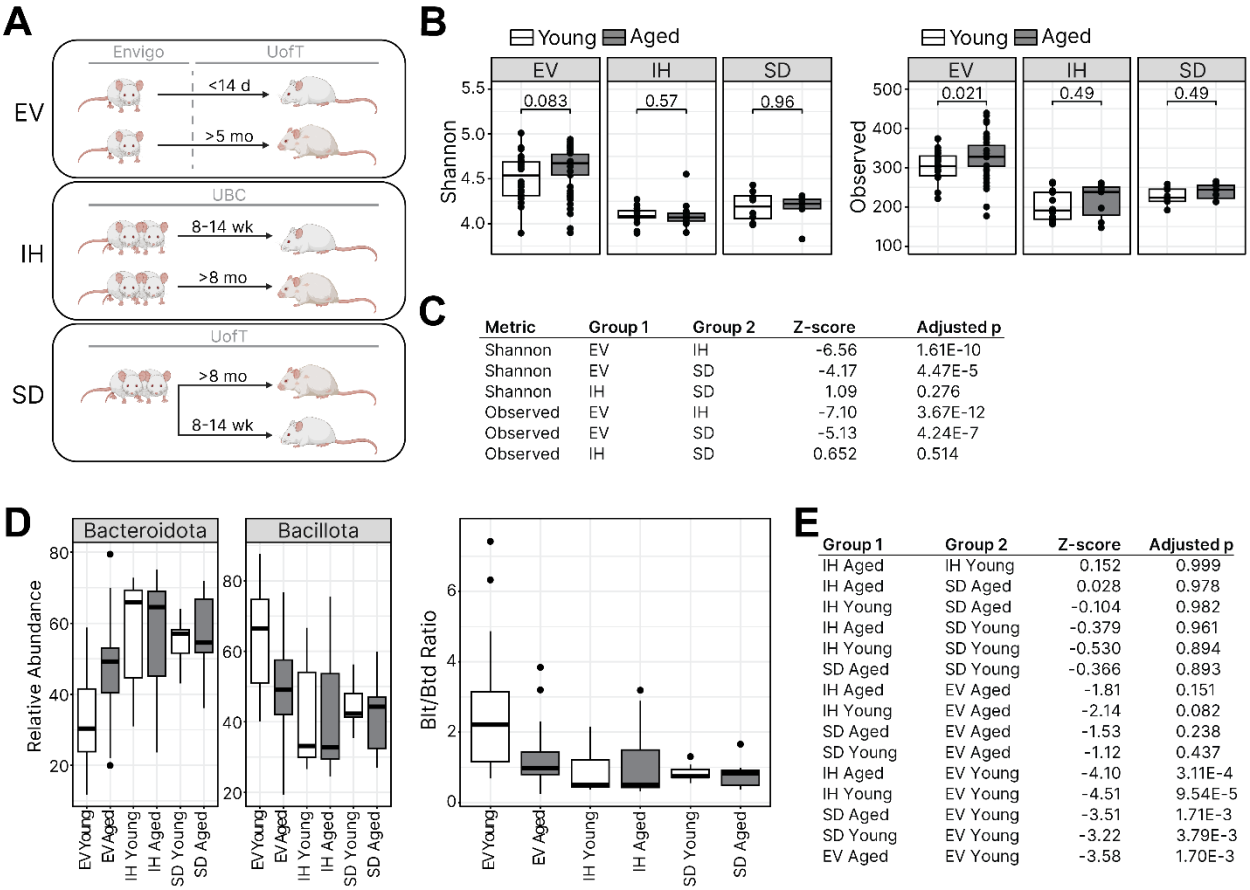

Metric	Group 1	Group 2	Z-score	Adjusted p
Shannon	EV	IH	-6.56	1.61E-10
Shannon	EV	SD	-4.17	4.47E-5
Shannon	IH	SD	1.09	0.276
Observed	EV	IH	-7.10	3.67E-12
Observed	EV	SD	-5.13	4.24E-7
Observed	IH	SD	0.652	0.514

Group 1	Group 2	Z-score	Adjusted p
IH Aged	IH Young	0.152	0.999
IH Aged	SD Aged	0.028	0.978
IH Young	SD Aged	-0.104	0.982
IH Aged	SD Young	-0.379	0.961
IH Young	SD Young	-0.530	0.894
SD Aged	SD Young	-0.366	0.893
IH Aged	EV Aged	-1.81	0.151
IH Young	EV Aged	-2.14	0.082
SD Aged	EV Aged	-1.53	0.238
SD Young	EV Aged	-1.12	0.437
IH Aged	EV Young	-4.10	3.11E-4
IH Young	EV Young	-4.51	9.54E-5
SD Aged	EV Young	-3.51	1.71E-3
SD Young	EV Young	-3.22	3.79E-3
EV Aged	EV Young	-3.58	1.70E-3

Figure 1. (A) Schematic of cohorts of mice sampled. Mice were either purchased from Envigo (EV), bred in-house but not arising from the same breeding pairs (IH), or sister litters arising from the same breeding pairs (SD). (B) Alpha diversity metrics of cohorts. (C) Comparison of inter-cohort differences in alpha diversity, independent of age. (D) Relative abundances of Bacteroidota and Bacillota phyla across all cohorts, and Bacillota-to-Bacteroidota ratio (Blt/Btd) calculated by dividing the relative abundance of Bacillota sequences by relative abundances of Bacteroidota sequences. (D) Relative abundances of detectable phyla. (E) Relative frequencies of the top 20 most abundant families across all samples. Young vs. aged alpha diversity comparison by Wilcoxon rank sum test. For all other statistical comparisons, Kruskal-Wallis with Dunn's post hoc test for multiple comparisons.

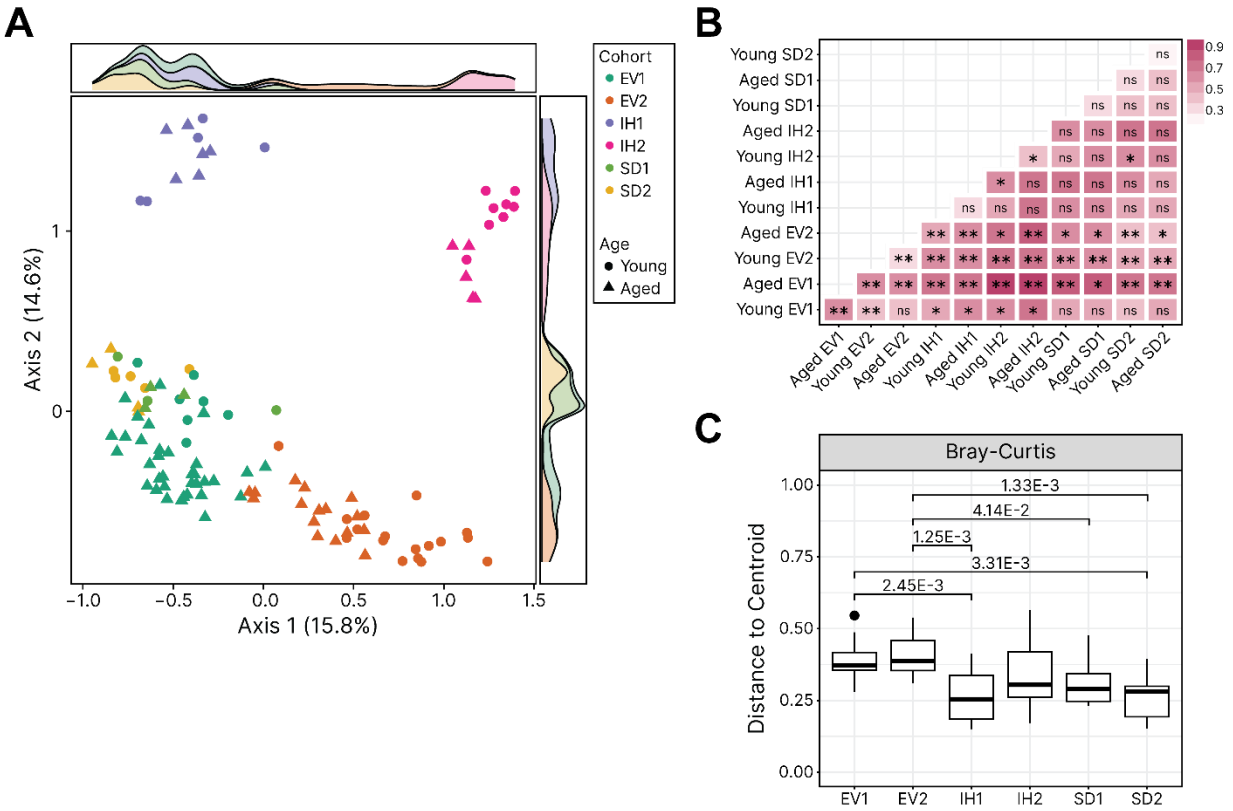

Figure 2. (A) Principal coordinate analysis (PCoA) plot using Bray-Curtis distances among all cohorts as described in Figure 1. Two independent batches of fecal pellets were collected from different groups of mice. (B) Pairwise comparisons of mean Bray-Curtis distances between agglomerated samples from young or aged mice. (C) Dispersion from the centroid for all cohorts. For (B), pairwise PERMANOVA, permutations = 9999 with p value adjustment using Holm method. For (C), Kruskal-Wallis test with Dunn's post hoc test.

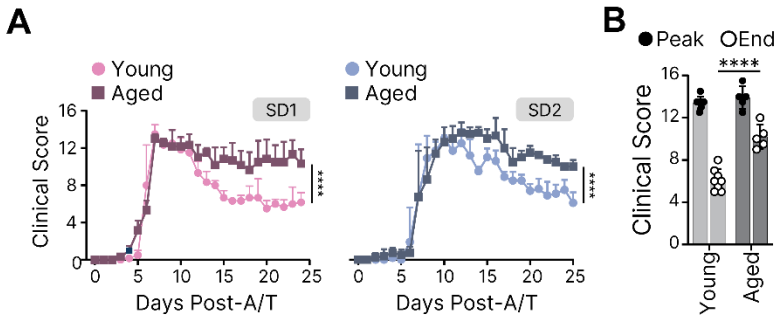

Figure 3. (A) EAE clinical score curves for independent experiments conducted in two sets (SD1, SD2) of young and aged mice born to the same dam (shown as SD in Figure 1A). n = 3 young and 3 aged (SD1), or 4 young and 5 aged (SD1). 2 young mice from SD2 died prior to the experimental endpoint. (B) Peak scores and endpoint scores for animals aggregated from both experiments. Two-way ANOVA with Tukey's post hoc test for multiple comparisons.

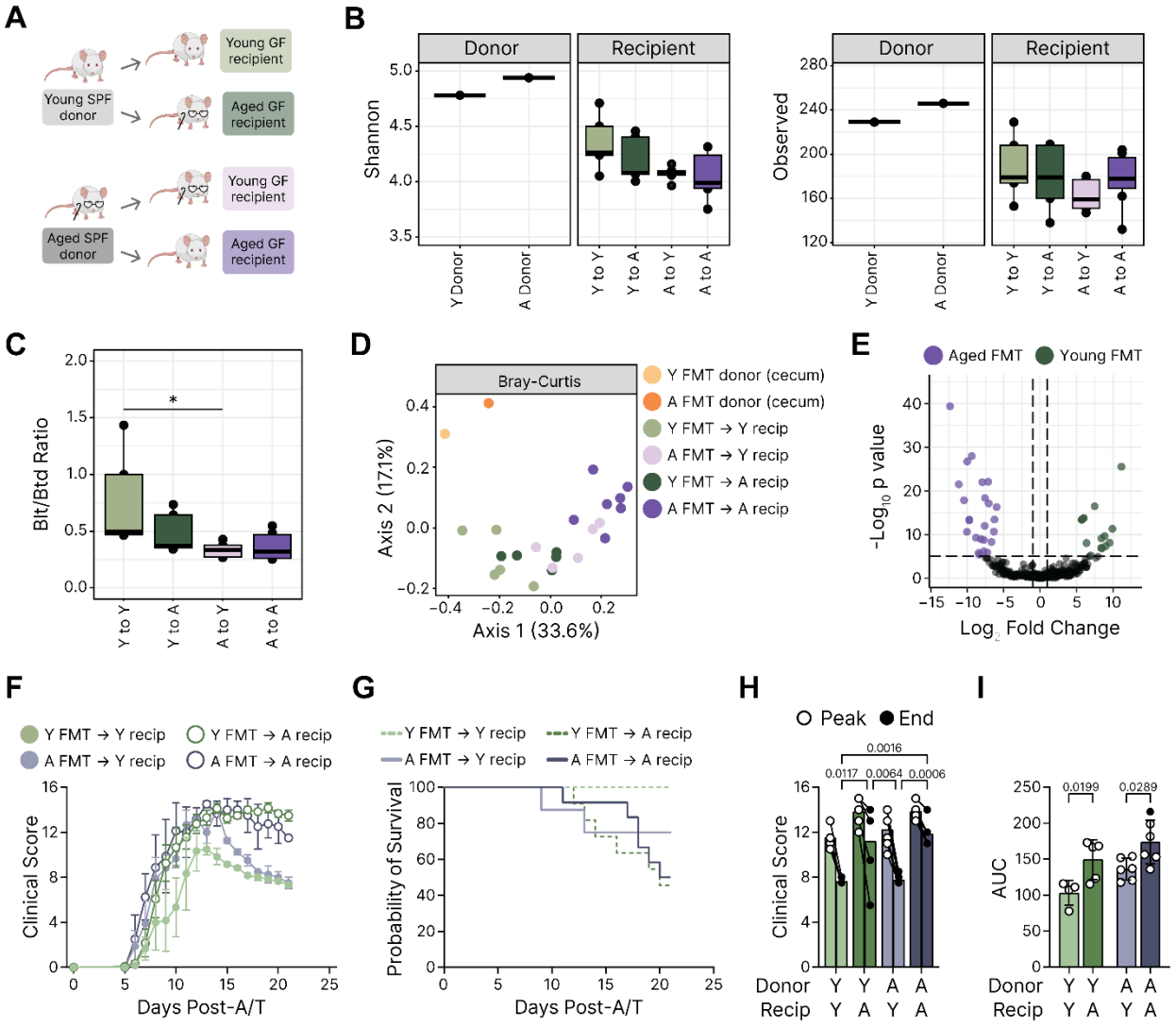

Figure 4. (A) Schematic of FMT donors and recipients. (B) Shannon and Inverse Simpson alpha diversity metrics of donor mouse cecal material and fecal pellets from recipient mice. (B) Shannon diversity (left) and total number of detected ASVs (right). (C) Blt/Btd ratios in all four groups of FMT recipient mice. (D) PCoA plot generated using Bray-Curtis distances. (E) Volcano plot indicating differentially abundant taxa found in aggregated recipients of either young or aged FMT. (F) EAE graph of young or aged GF mice receiving donor cecal material from young or aged SPF mice. (G) Kaplan-Meyer survival plot indicating deaths experienced in each experimental group. (H) Comparisons of peak and endpoint clinical scores across groups. (I) Area under the curve calculation for all groups, significance indicated represents overall effect of young vs. aged recipients. For (B) and (C), Kruskal-Wallis with Dunn's post hoc test for multiple comparisons. p value adjustment using Holm method. For (D), PERMANOVA, permutations = 999 with p value adjustment using Holm method. For (E), the DESeq2 package (version 1.42.0) was used. Adjusted p value threshold shown in plot is $1x10^{-4}$. For (H) and (I), Two-way ANOVA with Tukey's post hoc test for multiple comparisons.

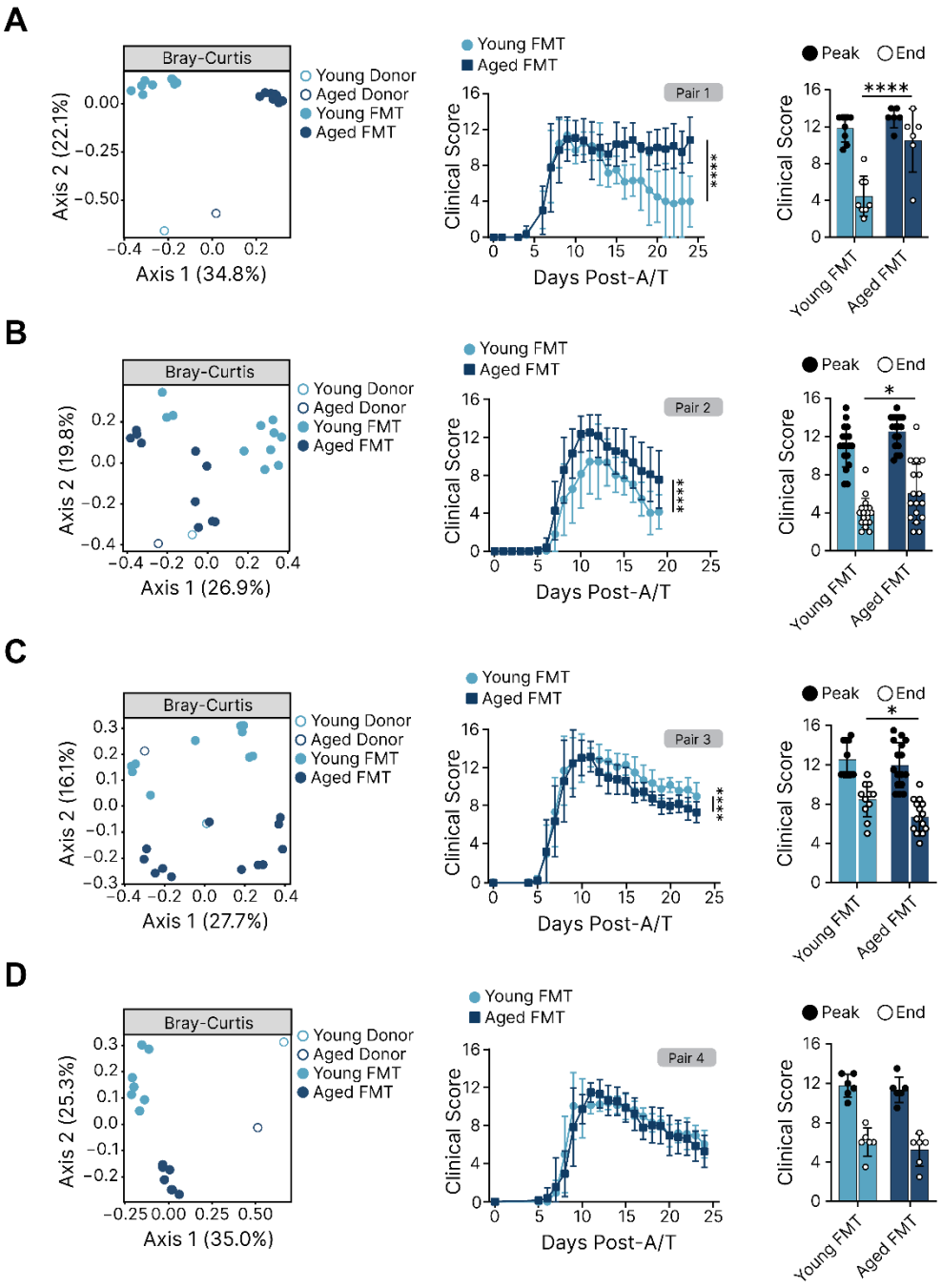

Figure 5. (A-D) Four human donor pairs assessed for EAE-modifying capacity. EAE curves (left), peak-endpoint analyses (middle), and PCoA plots displayed using Bray-Curtis distances (right). For PCoA plots, PERMANOVA (permutations = 999) excluding donor samples due to an n of 1 for each individual donor. For EAE curves and peak-end analysis, two-way ANOVA with Tukey post hoc test for multiple comparisons.

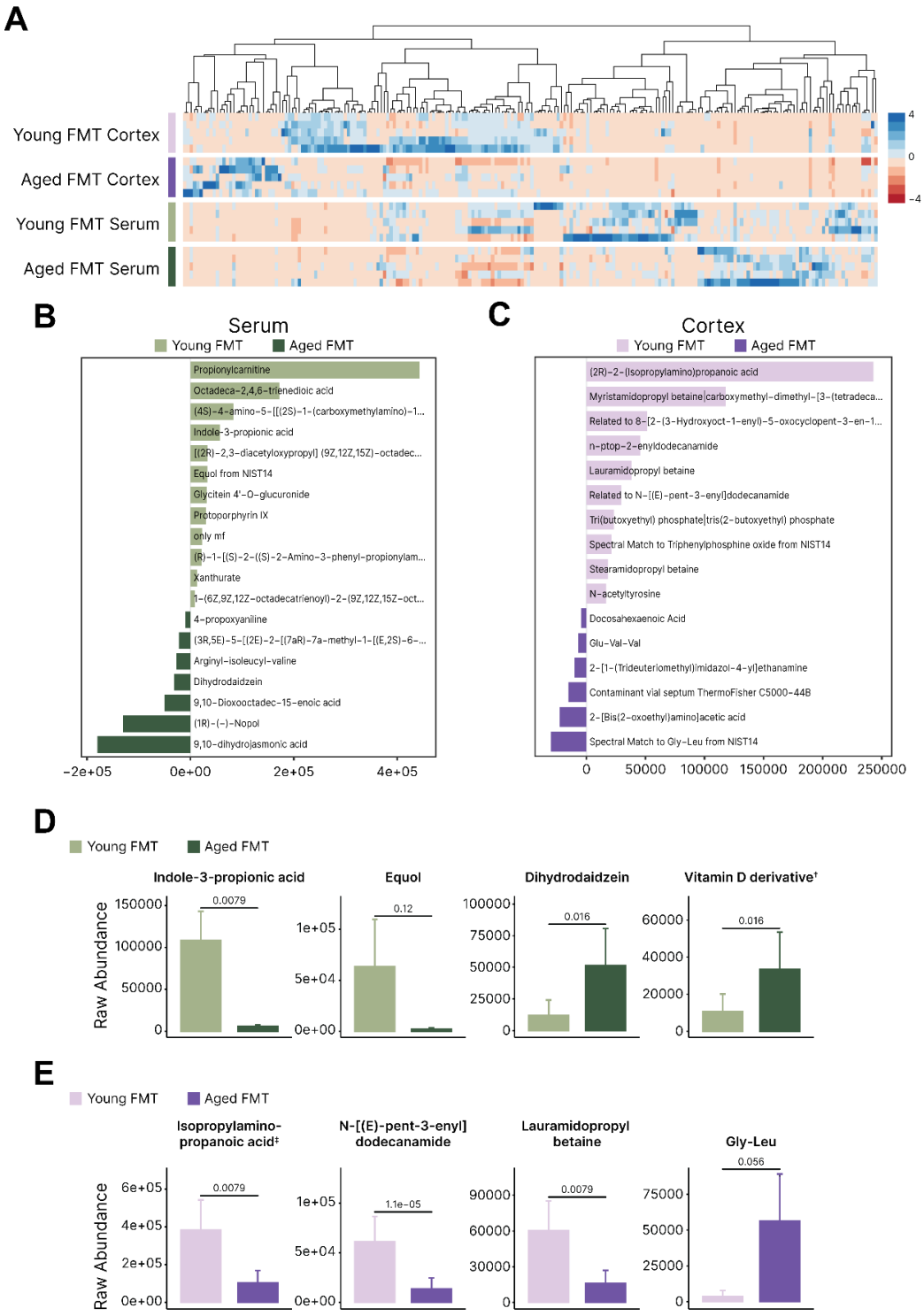

Figure 6. (A) Normalized heat map of compounds detected in cortex and serum samples from young or aged FMT mice. (B)(C) Selected metabolites that were differentially abundant between young or aged FMT serum (green) or young or aged FMT cortex (purple). Metabolite structures were proposed based on molecular formula and MS fragmentation patterns. (D)(E) Differential metabolites indicating dietary or other environmental differences. Wilcoxon rank sum test.

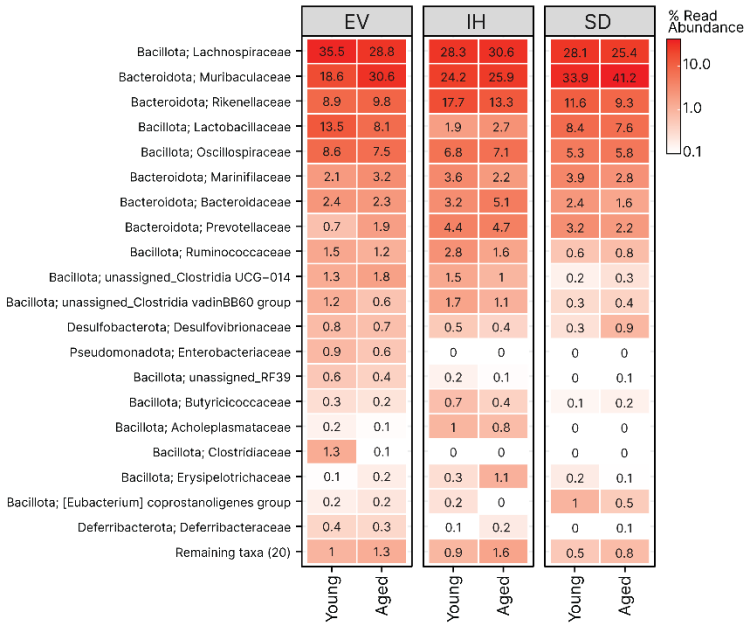

Figure S1. Heatmap of relative abundances of the top 20 most abundantly detected families.

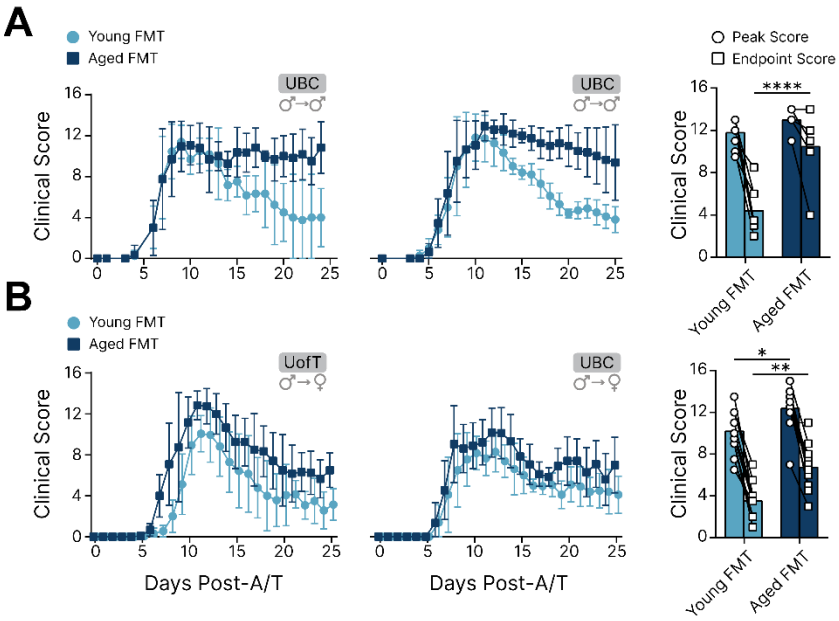

Figure S2. Independent experiments conducted at UBC and UofT vivariums in (A) male and (B) female recipient mice. Two-way ANOVA with Sidak's post hoc test for multiple comparisons.

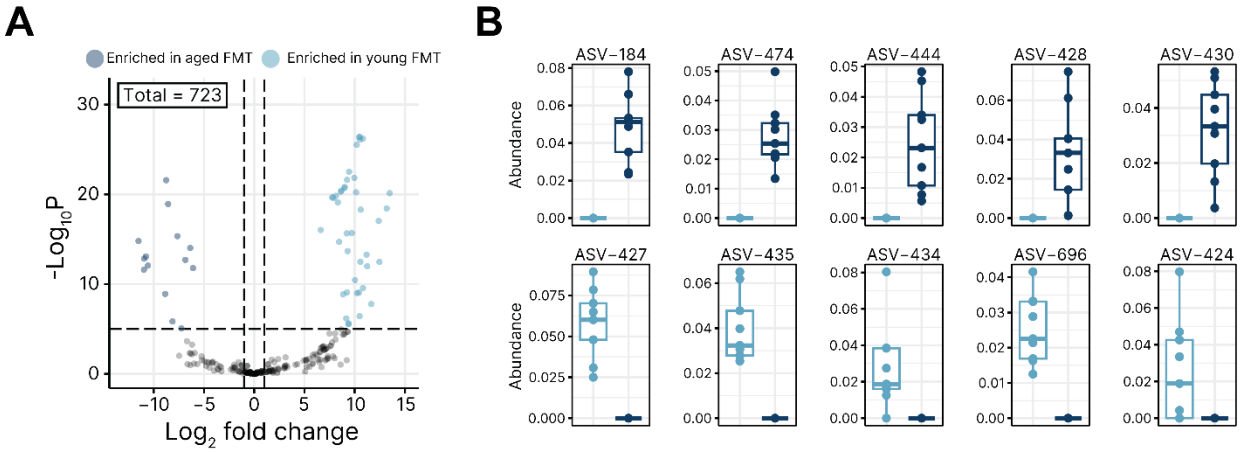

Figure S3. (A) Volcano plot of differentially abundant taxa as analyzed using DESeq2 between recipients of young or aged FMT from Pair 1 donor material. (B) Highlighted ASVs that are significantly enriched in young FMT (light blue) or aged FMT (dark blue). ASV-184 Fusobacterium ulcerans, ASV-474 Parabacteroides merdae, ASV-444 Bacteroides caccae, ASV-428 and ASV-430 Bacteroides sp., ASV-427 Bacteroides uniformis, ASV-435 Bacteroides nordii, ASV-434 Bacteroides sp., ASV-696 Bilophila wadsworthia, ASV-424 Akkermansia muciniphila.